

# New Measurements of the EMC Effect in Few-Body Nuclei

**J. Arrington**

Physics Division, Argonne National Laboratory, Argonne, IL 60639

For the JLab E03-103 collaboration.

E-mail: [johna@anl.gov](mailto:johna@anl.gov)

**Abstract.** Measurements of the EMC effect show that the quark distributions in nuclei are not simply the sum of the quark distributions of the constituent nucleons. However, interpretation of the EMC effect is limited by the lack of a reliable baseline calculation of the effects of Fermi motion and nucleon binding. We present preliminary results from JLab experiment E03-103, a precise measurement of the EMC effect in few-body and heavy nuclei. These data emphasize the large- $x$  region, where binding and Fermi motion effects dominate, and thus will provide much better constraints on the effects of binding. These data will also allow for comparisons to calculations for few-body nuclei, where the uncertainty in the nuclear structure is minimized.

## 1. Introduction

One topic of great interest in the study of Quantum Chromodynamics (QCD) is the question of whether or not the internal structure of nucleons is modified inside of the nuclear medium. Measurements of the “EMC effect” provide an unambiguous experimental indication that the quark distribution of a nucleus is not the naive sum of the quark distributions of the individual nucleons. However, there have been many explanations proposed for the EMC effect, some of which require a modification to the in-medium nucleon structure, and some of which do not. So while the experimental signature is clear, the interpretation of the effect is, at present, ambiguous.

One important issue in understanding the modification of the nuclear quark distributions at large Bjorken  $x$ , i.e. large quark momentum, is that binding and the Fermi motion of the nucleons must clearly play a significant role. While these contributions are usually discussed when describing the EMC effect at very large  $x$  values, binding leads to a modification of the distributions at all  $x$  values. Therefore, one must have a precise and quantitative understanding of these effects before one can determine from the data if additional, more exotic explanations must be invoked to describe the data.

The bulk of the measurements of nuclear parton distributions are for heavy nuclei,  $A \gtrsim 12$ , where there are uncertainties in the details of the nuclear structure that go into determining the effect of binding. In addition, there is very little data above  $x = 0.8$ , where binding effects should dominate. This is the region where high precision data could be used to evaluate calculations of binding, and yet the data in this region is of limited precision. Because of the lack of data to constrain the effects of binding and the limited data for few-body nuclei, where nuclear structure uncertainties are minimized, many calculations of the EMC effect are performed for nuclear

matter, and extrapolated to lower density when comparing to the nuclear parton distributions. In this case, it is difficult to be certain that the “traditional” effects of binding and Fermi motion are modeled well enough to examine the effect of more exotic effects, such as the contributions of nuclear pions or modification of the nucleon structure.

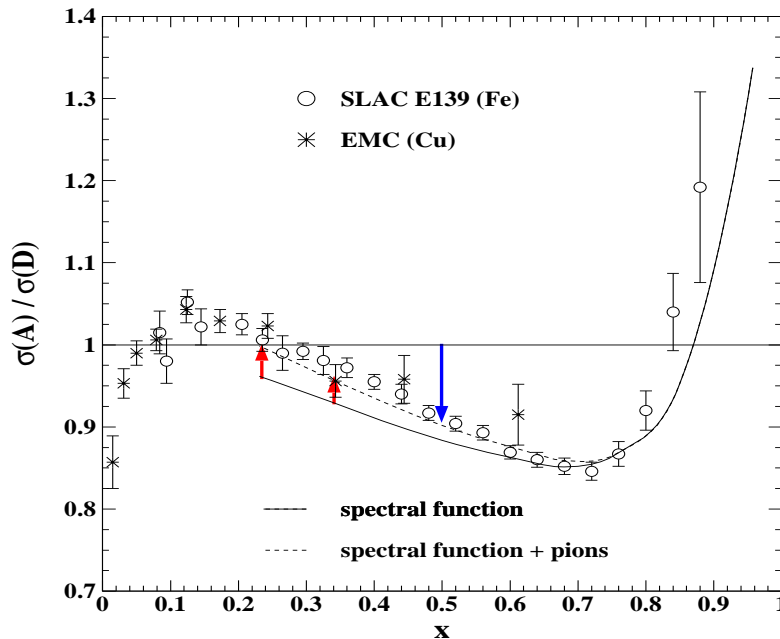


**Figure 1.** Existing data for the EMC effect for nuclei near Fe [1, 2], along with two calculations by Benhar, Pandharipande and Sick [3]. The solid line is their binding-only calculation, while the dotted line includes their calculation of the contribution from nuclear pions.

Figure 1 shows one example of a detailed binding calculation [3]. The solid line indicates the result including only binding, and based on this calculation, one expects that any additional exotic effects must lead to a small enhancement of the parton distributions for  $x \lesssim 0.5$ , as indicated by the red arrows. In Ref. [3], the authors include the contributions of so-called “nuclear pions” to explain the additional enhancement needed at small  $x$  values. This is in contrast to models that use a more exotic explanation to explain the full EMC effect, including all of the suppression of the quark distributions for the larger  $x$  values, as indicated by the blue arrow.

Note that the binding calculation in Fig. 1 does not reproduce even the somewhat low precision data at very large  $x$ , and therefore is not fully explaining the effects of binding. More precise data in this region, especially for light nuclei where the uncertainties in the nuclear structure are smaller, will allow for precise tests of the binding calculations that serve as a necessary baseline when looking for additional contributions.

Previous measurements were limited at large  $x$  values because of the requirement that the data be taken in the deep inelastic scattering (DIS) regime. The requirement that data be limited to large  $W^2$ , where  $W$  is the invariant mass of the unobserved hadronic system, meant that the data had to be taken at very large  $Q^2$  for large  $x$  values. For the usual DIS condition,  $W^2 > 4 \text{ GeV}^2$ ,  $Q^2$  must be above  $18 \text{ GeV}^2$  for  $x = 0.85$ , limiting the range of the measurements as the cross sections fall rapidly with both  $x$  and  $Q^2$ . Recent measurements of inclusive scattering from nuclei [4, 5] indicate that the scaling of the nuclear structure function expected in the DIS regime extends to lower  $W$  values. By relaxing the constraint on  $W^2$ , large  $x$  data can be

accessed at significantly lower  $Q^2$ , and thus larger  $x$  values can be accessed. For  $x = 0.85$ , the minimum  $Q^2$  is reduced to 12 (9)  $\text{GeV}^2$  for  $W^2 > 3$  (2.5)  $\text{GeV}^2$ . Limited measurements of the EMC effect at lower  $W^2$  suggest that the scaling continues to even lower  $W^2$  and  $Q^2$  values [6].

## 2. Experimental details

Jefferson Lab (JLab) experiment E03-103 [7] took data on few-body and heavy nuclei, with an emphasis on the large- $x$  region, with the goal of providing high precision data that can be used to evaluate detailed calculations of the effects of binding. Such calculations can then provide a much more reliable baseline when evaluating additional contributions to the nuclear parton distributions at lower  $x$  values.

The experiment was run in Hall C at Jefferson Lab during the summer and fall of 2004. The bulk of the data were taken at a beam energy of 5.8 GeV, with beam currents ranging from 30 to 80  $\mu\text{A}$ . Data were taken on cryogenic  $^1\text{H}$ ,  $^2\text{H}$ ,  $^3\text{He}$ , and  $^4\text{He}$ , as well as solid Be, C, Al, Cu, and Au targets. For the main measurements, scattered electrons were detected in the High Momentum Spectrometer (HMS). The HMS has a solid angle of approximately 6.8 msr, momentum acceptance of roughly  $\pm 9\%$ , and can detect scattered electrons with momenta up to the beam energy. Electrons are separated from pions using cuts on the gas Cerenkov and lead-glass shower counter, which leave a negligible contribution of pions.

Data for all targets was taken at  $40^\circ$  and  $50^\circ$  electron scattering angle, corresponding to  $Q^2$  values near 3  $\text{GeV}^2$  at  $x = 0.3$  and 6  $\text{GeV}^2$  at  $x = 0.9$ . Because some of this data is below the typical DIS limit ( $W^2 > 4 \text{GeV}^2$ ), we took additional data on the  $Q^2$  dependence for Carbon and Deuterium, covering six angles between  $18^\circ$  and  $50^\circ$  at a beam energy of 5.8 GeV, and four additional angles at 5.0 GeV. This allows us to verify that the structure function shows precise scaling in this region, as suggested by previous data [4, 5, 6], as well as directly verifying that the extracted EMC ratios are independent of  $Q^2$ . Figure 2 shows the kinematics for the measurement. Carbon and deuterium data were taken at all settings shown, while the other targets were measured only for the two largest  $Q^2$  settings.

The high luminosity and large acceptance spectrometers in Hall C, coupled with high density cryogenic  $^3\text{He}$  and  $^4\text{He}$  targets, allowed high precision measurements of the target ratios for both the few body nuclei and the large  $x$  region. The largest limitation is the fact that the high  $Q^2$  data is taken at large scattering angle, due to the beam energy. This leads to some corrections being larger than for previous measurements at higher energy. First, one detects both scattered electrons and electrons that come from the production of positron-electron pairs. These secondary electrons cannot be separated from the beam electrons that scatter in the target. The contribution from this charge-symmetric background (CSB) can be quite large for the large scattering angle, especially for very low  $x$  values and the high- $Z$  targets. Data was taken for both positive and negative polarity, allowing a direct measurement of the CSB. For the worst case conditions, the heavy targets (Cu and Au) at  $50^\circ$  and large energy transfer (small  $x$ ), the contribution from the charge-symmetric background can be as large as the signal from scattered electrons. However, this background is a factor of three lower for lighter nuclei, and also decreases rapidly with scattering angle, and so is an order of magnitude smaller for the lighter nuclei at  $40^\circ$ . Comparisons of the  $40^\circ$  and  $50^\circ$  data on Au indicate that the uncertainty due to the subtraction on the CSB is reasonably small ( $< 5\%$ ), even when the correction itself is 100%. Thus this is a small contribution to the uncertainty for the majority of the data, especially for the few-body nuclei.

In addition, the data at large scattering angle ends up having non-trivial corrections due to Coulomb distortion. These corrections are estimated to be up to 10% for the Au data at  $50^\circ$  and very small  $x$  values, according to the updated effective momentum approximation prescription of Ref. [8]. Again, these corrections are much smaller for lighter nuclei and for smaller scattering angles, and so again will have a small contribution to the final uncertainty, except for the worst

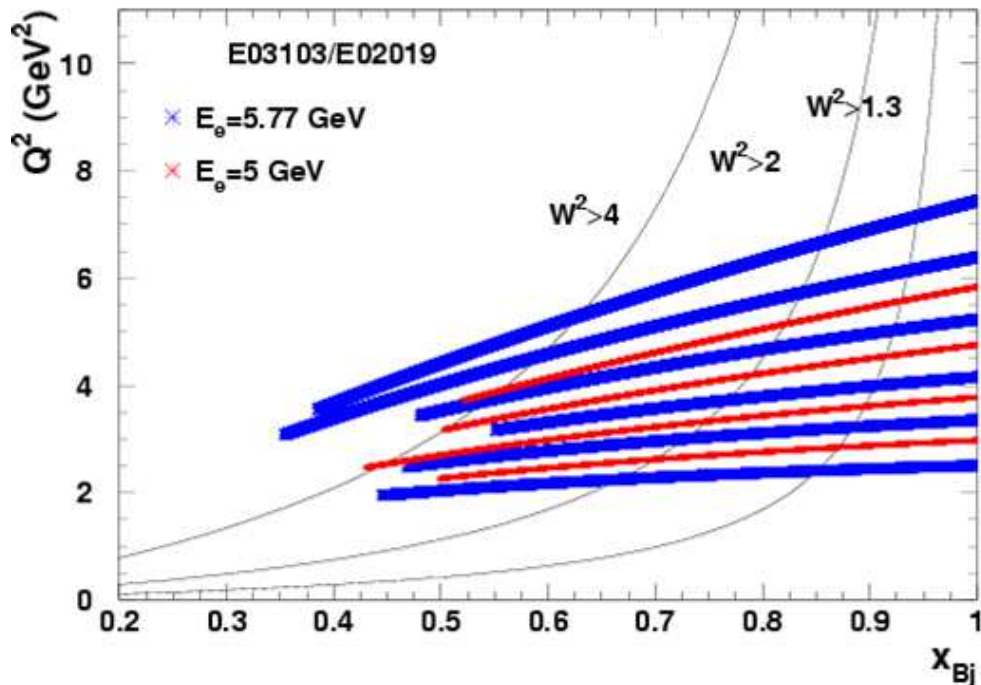


**Figure 2.** The kinematics for the deuterium and carbon running for E03-103. Other targets were taken only at the two highest  $Q^2$  settings. The results from Ref. [6] were taken between  $Q^2 = 3 \text{ GeV}^2$  at  $x = 0.6$  and  $Q^2 = 4 \text{ GeV}^2$  at  $x = 0.9$ .

case conditions mentioned above. Finally, radiative corrections can be quite large for the small  $x$  data at large scattering angles, and this correction is sensitive to the model of the quasielastic cross section at low  $Q^2$ . Detailed tests of the model dependence are underway, and this is not expected to be a limiting factor for any of the kinematics.

There are two main advantages to this experiment, compared to previous measurements of the EMC effect. First, the high density cryogenic Helium targets allowed for much higher luminosity than available with the internal  $^3\text{He}$  target at HERMES [9]. The luminosity was also noticeably larger than for the  $^4\text{He}$  data from SLAC E139 [2] and with much smaller target density fluctuations due to beam heating. Second, by taking data at  $W^2$  values slightly below the usual DIS cut of  $4 \text{ GeV}^2$ , we were able to take data at large  $x$  with much higher statistics. Previous measurements have observed that the nuclear structure functions show extended scaling in the Nachtmann variable  $\xi$  well below the usual DIS region [4, 10, 5]. It was also shown that in the target ratios, the results were in agreement with the DIS measurements even for  $Q^2 \approx 3\text{--}4 \text{ GeV}^2$  and  $W^2$  values from  $1.3\text{--}2.8 \text{ GeV}^2$  [6].

This can be understood as a consequence of quark-hadron duality in the unpolarized nucleon structure functions [11, 12]. It was observed originally by Bloom and Gilman [13] that while the proton inclusive structure function in the resonance region shows structure due to the individual resonance contributions, the structure function is, on average, in agreement with the DIS limit. Thus, integrating over the region of a prominent resonance yields the same result as integrating over the equivalent region in the DIS limit. In a nucleus, the Fermi motion provides this averaging, so rather than seeing a duality between the resonance region structure function when

averaged over a range in  $W^2$ , we see that the structure function in the resonance region is identical to the DIS limit, after taking into account QCD evolution and target mass corrections. In these and other previous studies of duality in inclusive electron scattering, the target mass corrections were often approximated by taking the data as a function of Nachtmann  $\xi$ , or some other variable, rather than Bjorken- $x$ . While this approximation works well, duality studies have also been performed with explicit target mass corrections [14, 12, 15].

### 3. Preliminary results

We have extracted preliminary cross sections and EMC ratios for all of the targets, but will focus here on the light nuclei, where the charge-symmetric background and Coulomb distortion corrections are much smaller. As discussed in the previous section, we expect that the data should show scaling in  $\xi = 2x/(1 + \sqrt{1 + 4m_p^2x^2/Q^2})$ , even though some of the data is below  $W^2 = 4 \text{ GeV}^2$ . Note that the difference between  $x$  and  $\xi$  goes like  $x^2/Q^2$ , and so for small  $x$  or very large  $Q^2$ ,  $\xi \rightarrow x$ . Thus, for the very high energy measurements focussed on low  $x$ , the result is identical for  $x$  or  $\xi$ . For large  $x$  values, there can be a noticeable difference between  $x$  and  $\xi$ . In the target ratios, this is simply a shift from  $x$  to  $\xi$ , and so only the shape of the EMC effect will change when plotted as a function of  $\xi$  rather than  $x$ . This shift is nearly identical for both this measurement and the SLAC E139 result, shifting data at  $x = 0.8$  to  $\xi \approx 0.7$ , while having a small effect for  $x < 0.5$ . As these are the only measurements with significant data at large  $x$ , we show our results as a function of  $x$ , rather than  $\xi$ , so that they can be directly compared to previously extracted EMC ratios and calculations.

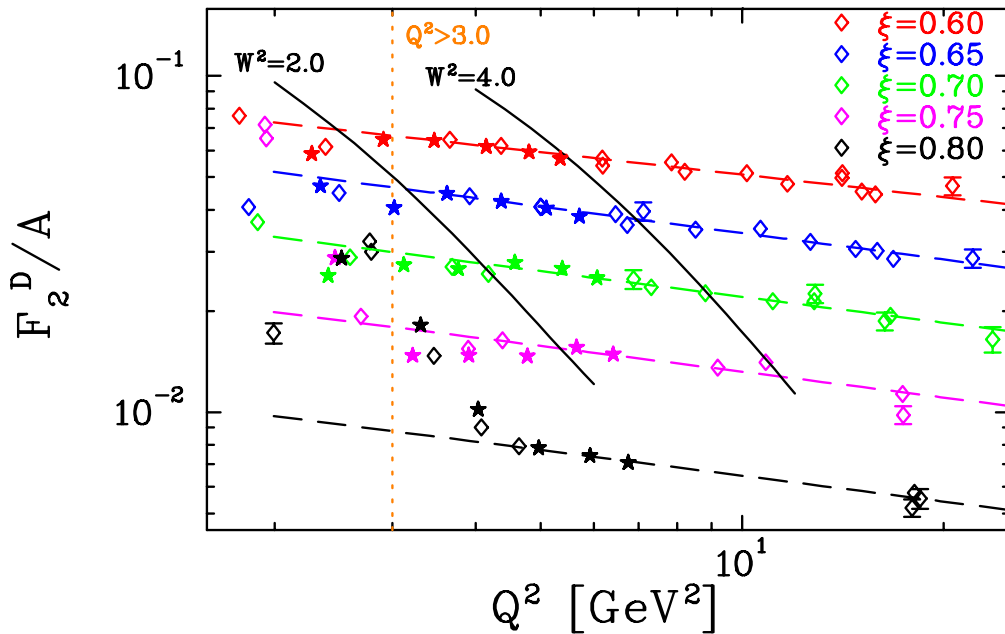


**Figure 3.** The  $Q^2$  dependence of the deuteron structure function at fixed  $\xi$  values. The hollow points are previous SLAC and JLab data, while the solid stars are the preliminary E03-103 results. The dashed lines correspond to fixed values of  $d \ln(F_2)/d \ln(Q^2)$ , fit to the large  $Q^2$  SLAC data. The structure function is consistent with this evolution well below the DIS limit, down to  $W^2 = 2$  for the  $\xi$  values shown here.

The measurements are in the DIS region up to  $x \approx 0.65$ . For larger  $x$  values, we rely on the extended scaling in nuclei. We observe that the structure functions for carbon and deuterium

are consistent with the prediction of QCD evolution at better than the 5% percent level over most of the range of the data, including over most of the resonance region at the higher  $Q^2$  values from this measurement (see Fig. 3). While we do not see deviations from QCD scaling in the individual structure functions, any deviations that are too small to see will be suppressed to the extent that they are  $A$ -independent.

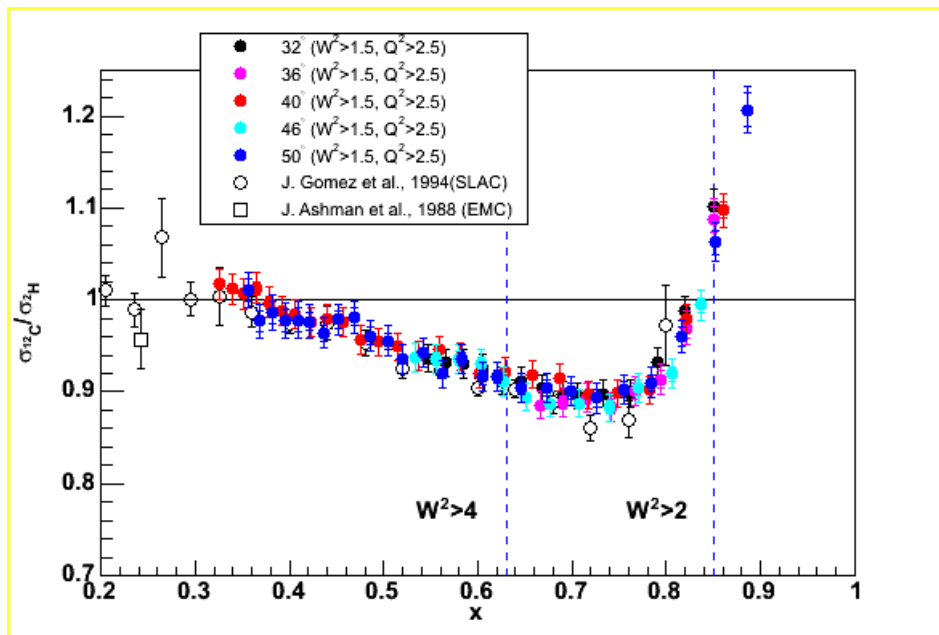


**Figure 4.** Preliminary EMC ratios from E03-103 for  $^{12}\text{C}$  (top) for the five largest  $Q^2$  settings of the experiment. The extracted EMC ratios are consistent within the uncertainties for all settings, and there is no systematic  $Q^2$  dependence, up to  $x = 0.85$ . Hollow points are data from previous measurements [1, 2].

A more precise test is made by examining the  $Q^2$  dependence of the EMC ratio, where many of the systematic uncertainties cancel in the ratio. Figure 4 shows the  $Q^2$  dependence of the EMC ratio for carbon for the five largest  $Q^2$  values taken during the experiment - three at 5.8 GeV beam energy, and two ( $36^\circ$  and  $46^\circ$ ) at 5.0 GeV. The EMC ratios are very precise, and are independent of  $Q^2$  over the entire range of  $x$ . While the  $Q^2$  dependence of the structure functions is quite different when taken at fixed  $x$  as opposed to fixed  $\xi$ , the effect on the target ratios is extremely small, and the EMC ratios are independent of  $Q^2$  whether taken as a function of  $x$  or  $\xi$ .

The detailed measurements of the  $Q^2$  dependence were only taken for Carbon and Deuterium. For the extraction of the EMC effect, we limit ourselves to the two data sets at the largest  $Q^2$  values. These are the  $40^\circ$  and  $50^\circ$  settings taken with a beam energy of 5.8 GeV, where data was taken for all nuclei. Figure 5 shows the preliminary results for extracted EMC ratios for  $^{12}\text{C}$  and  $^4\text{He}$ . For these isoscalar nuclei, the cross section ratios are identical to the usual EMC ratios, assuming that  $R = \sigma_L/\sigma_T$  is  $A$ -independent. The  $^{12}\text{C}$  EMC ratio is consistent with previous data, but of much higher precision at large  $x$  values, where previous measurements were statistics limited, mainly due to the large  $Q^2$  values required to reach the DIS regime. While the SLAC data suggested that the EMC effect in  $^4\text{He}$  was slightly smaller than for  $^{12}\text{C}$ , these new results indicate that the EMC is nearly identical to the  $^{12}\text{C}$  data. The average density of  $^4\text{He}$  is anomalously large for such a light nucleus, and is in fact nearly identical to the average

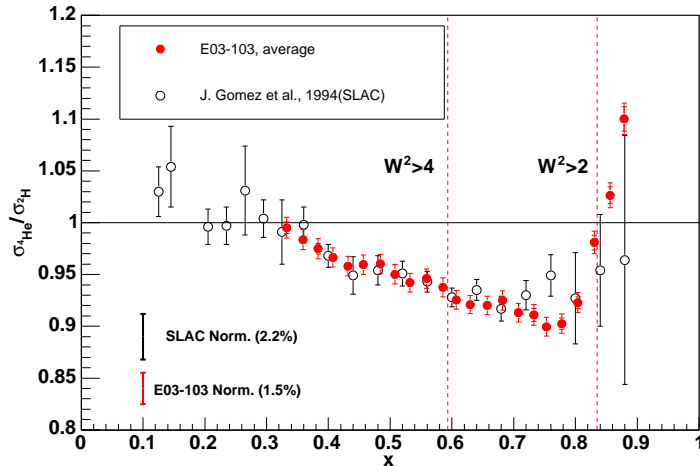
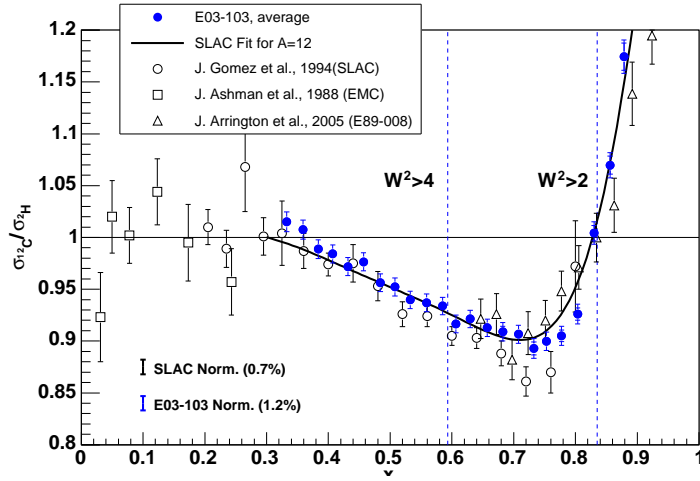


**Figure 5.** Preliminary EMC ratios from E03-103 for the  $^{12}\text{C}$  (top),  $^4\text{He}$  (bottom). Inner error bars are statistical, while the outer error bars are the combined statistical and estimated systematic uncertainty. The hollow points are data from previous measurements [1, 2, 6]. Error bars in the lower left corner of each plot indicate the estimated normalization uncertainty of the previous and present measurements.

nuclear density for  $^{12}\text{C}$ , so these preliminary results are consistent with models where the EMC effect scales with the nuclear density.

The results for  $^3\text{He}$ , shown in Figure 6 do not provide the same *direct* measure of the EMC effect for  $A = 3$ . Because  $^3\text{He}$  has two protons and one neutron, we must apply a correction for the proton excess to obtain the isoscalar EMC ratio, and there is uncertainty in the neutron cross section in this region. The blue squares show the uncorrected cross section ratio, while the green circles show the result after correcting for the proton excess using the same fit as for SLAC E139:  $\sigma_n/\sigma_p = 1 - 0.8x$ . The correction for  $^3\text{He}$  is nearly identical, but of the opposite sign, to the correction applied to Au, which has a large neutron excess. The correction can be quite large, and the extracted EMC ratio can change by several percent if one uses a different parameterization for the ratio  $\sigma_n/\sigma_p$ . Thus, the interpretation of the  $^3\text{He}/^2\text{H}$  ratio is dependent on the assumed isoscalar correction. Because we also took data on  $^1\text{H}$ , we can extract the ratio of  $^3\text{He}$  to  $(^1\text{H} + ^2\text{H})$ , which does not rely on having a model for  $\sigma_n/\sigma_p$ . Because comparing to the deuteron takes into account a significant portion of the Fermi motion correction, which is significant at the largest  $x$  values, the  $x$  dependence of this ratio will look quite different than the usual isoscalar corrected ratios. However, it can be more directly compared to calculations.

We are also examining extractions of the neutron cross section in this region, and will be able to estimate the uncertainty in the  $A = 3$  EMC effect, both by examining the uncertainties in  $\sigma_n/\sigma_p$  and by examining the  $A$  dependence of the EMC effect. An isoscalar correction that significantly increases the EMC effect for  $A = 3$  would have an equal but opposite effect for

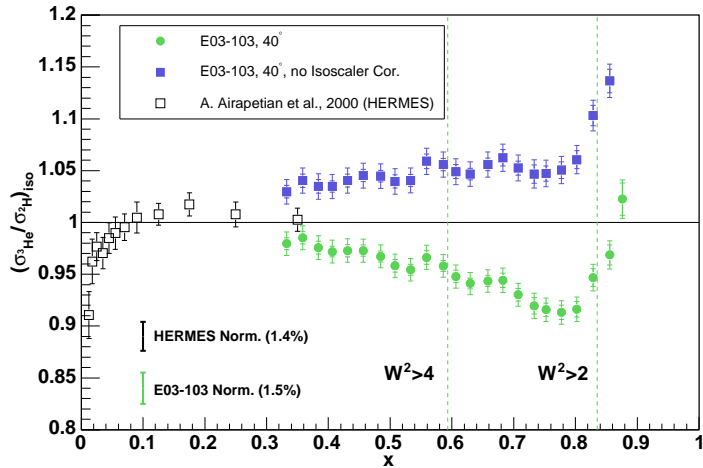


**Figure 6.** Preliminary EMC ratios from E03-103 for the  ${}^3\text{He}$ , errors are the same as in Fig. 5. The hollow points are data from previous measurements [9]. The blue squares show the raw  ${}^3\text{He}/{}^2\text{H}$  cross section ratio, while the green circles show the ratios corrected to an isoscalar  $A = 3$  nucleus, taking the ratio of  $\sigma_n/\sigma_p$  from the SLAC fit used in Ref. [2].

Au, and so one can make a “sanity check” on the  $A$  dependence resulting from different models of the isoscalar correction. In addition, a consistency check can be performed by fitting the data for  $A=1-4$ , if one has a model of both  $\sigma_n/\sigma_p$  and the EMC effect. However, one cannot yet make an unambiguous separation between these two effects. A new experiment [16] was recently completed at Jefferson Lab which was designed to measure inclusive scattering from the neutron using a deuteron target and tagging a slow, backwards proton to identify events where the electron struck an effectively “free” neutron. This will provide further constraints on the correction to the  ${}^3\text{He}$  EMC ratios.

While there is a large uncertainty in the present extraction of the  $A = 3$  EMC effect, this preliminary data suggest that the EMC effect for  ${}^3\text{He}$  may be larger than one would expect if one simply scales the EMC effect by nuclear mass or average nuclear density. In either of these cases, one expects a much smaller effect for  $A = 3$  than observed in Carbon. This suggests the possibility that the EMC effect in the deuteron may also be larger than expected. However, additional study of the isoscalar correction is needed before one can make any significant conclusions from the  ${}^3\text{He}$  measurements.

#### 4. Conclusions

We have presented preliminary results for the EMC effect in light nuclei. The EMC effect for  ${}^4\text{He}$  is nearly identical to that for  ${}^{12}\text{C}$ , indicating that the modification of the quark distribution scales with the average nuclear density. The data for  ${}^3\text{He}$  suggest that the EMC effect may also be large for  $A = 3$  systems, but the interpretation depends on the model of the neutron cross section used to form the ratio of isoscalar nuclei.

Results for the heavier nuclei will soon be available, which will allow us to examine the  $A$  dependence of the EMC effect at large  $x$ , as well as examine the effect of the isoscalar correction on the  $A$  dependence. In addition, we will be able to provide the ratio of  ${}^3\text{He}$  to the sum of proton plus deuteron, avoiding the model dependence associated with the neutron cross section correction. Finally, we will provide a more detailed examination of the scaling of the nuclear structure function, both in the kinematic region discussed here, and for the  $x > 1$  region [17].

#### Acknowledgments

This work was supported in part by the U.S. Department of Energy, Office of Nuclear Physics, under contracts DE-AC02-06CH11357. The Thomas Jefferson National Accelerator Facility is operated by the Southeastern Universities Research Association under DOE contract DE-AC05-84ER40150.



- [1] J. Ashman *et al.*, Phys. Lett. **B202**, 603 (1988).
- [2] J. Gomez *et al.*, Phys. Rev. D **49**, 4348 (1994).
- [3] O. Benhar, V. R. Pandharipande, and I. Sick, Phys. Lett. **B469**, 19 (1999).
- [4] B. W. Filippone *et al.*, Phys. Rev. C **45**, 1582 (1992).
- [5] J. Arrington *et al.*, Phys. Rev. C **64**, 014602 (2001).
- [6] J. Arrington *et al.*, Phys. Rev. **C73**, 035205 (2006).
- [7] J. Arrington and D. Gaskell, spokespersons, Jefferson lab experiment E03-103, [http://www.jlab.org/exp\\_prog/generated/apphallc.html](http://www.jlab.org/exp_prog/generated/apphallc.html).
- [8] A. Aste, C. von Arx, and D. Trautmann, Eur. Phys. J. **A26**, 167 (2005).
- [9] K. Ackerstaff *et al.*, Phys. Lett. **B475**, 386 (2000).
- [10] J. Arrington *et al.*, Phys. Rev. C **53**, 2248 (1996).
- [11] I. Niculescu *et al.*, Phys. Rev. Lett. **85**, 1186 (2000).
- [12] W. Melnitchouk, R. Ent, and C. Keppel, Phys. Rept. **406**, 127 (2005).
- [13] E. D. Bloom and F. J. Gilman, Phys. Rev. Lett. **25**, 1140 (1970).
- [14] Y. Liang *et al.*, nucl-ex/0410027 (2004).
- [15] F. M. Steffens and W. Melnitchouk, Phys. Rev. **C73**, 055202 (2006).
- [16] H. Fenker, C. E. Keppel, S. Kuhn, and W. Melnitchouk, spokespersons, Jefferson lab experiment E03-012, [http://www.jlab.org/exp\\_prog/generated/apphallb.html](http://www.jlab.org/exp_prog/generated/apphallb.html).
- [17] J. Arrington, D. Day, B. Filippone, and A. F. Lung, spokespersons, Jefferson lab experiment E02-019, [http://www.jlab.org/exp\\_prog/generated/apphallc.html](http://www.jlab.org/exp_prog/generated/apphallc.html).